

# Sour-Resistant Line Pipe Steel Preventing Local Hard Zone for Severe Sour Service

Taishi FUJISHIRO\*  
Masahiko HAMADA  
Takuya HARA

Nobuyuki YOSHIMURA  
Taro MURAKI

## Abstract

*In the oil and gas industry, pipelines for natural gas transportation are exposed to wet H<sub>2</sub>S environments (sour environments) in some cases. Sulfide stress cracking (SSC), a type of hydrogen embrittlement, is a major issue for line pipes exposed to sour environments. There are some guidelines on the test methods and material requirements for low-alloy carbon steel used in sour environments and sour-resistant line pipes with SSC resistance have been developed. However, SSC occurred in sour-resistant line pipes used for high-pressure H<sub>2</sub>S environments. This paper describes recent research efforts to develop low-alloy steels for line pipes that can be used in high-pressure H<sub>2</sub>S environments from the viewpoints of hardness criteria for SSC susceptibility, hydrogen absorption, microstructure, and steel manufacturing technology.*

## 1. Introduction

Pipelines used for transporting oil and natural gas are often exposed to corrosive environments (sour environments), which contain hydrogen sulfide (H<sub>2</sub>S) gas. The presence of H<sub>2</sub>S in the sour environment promotes hydrogen entry into steel owing to the catalytic action of H<sub>2</sub>S. A sour environment is the most severe environment for hydrogen embrittlement. Compared to other types of hydrogen embrittlement that occur in an atmospheric corrosive environment (e.g., delayed fracture of high-strength bolt steel), hydrogen embrittlement of line pipes also occurs in low-strength steel. Hydrogen that permeates into steel from the sour environment causes hydrogen embrittlement, such as hydrogen-induced cracking (HIC), sulfide stress cracking (SSC), and stress-oriented hydrogen-induced cracking (SOHIC).<sup>1,2)</sup> SSC began to become a problem around 1950<sup>3)</sup> and was subsequently actively studied. In 1943, the National Association of Corrosion Engineers (NACE) was established to solve the problems of corrosion and cracking in sour environments. Activities at the NACE led to the development of the prototype material selection standard NACE MR0175/ISO 15156<sup>4)</sup> for sour environments in 1975, the test method NACE TM0177<sup>5)</sup> for evaluating the cracking resistance of materials in sour environments in 1977, and the four-point bending test method NACE TM0316<sup>6)</sup> in 2016.

In 2021, the NACE merged with the Society for Protective Coatings (SSPC) to become the Association for Materials Protection and Performance (AMPP). The current AMPP continues to revise the NACE standards.

Studies have shown that the susceptibility to SSC is influenced by the H<sub>2</sub>S partial pressure (pH<sub>2</sub>S) and the hardness of steel.<sup>7,8)</sup> As the pH<sub>2</sub>S and steel hardness increase, the SSC susceptibility also increases, as illustrated in **Fig. 1**. NACE MR0175/ISO 15156 provides the regions of environmental severity with respect to the SSC of carbon and low-alloy steels (**Fig. 2**). Low-alloy carbon steel must possess properties such as yield strength and hardness that correspond to the severity of the sour environment. Regions 1, 2, and 3 are divided based on experimental SSC test results.<sup>9)</sup> The upper hardness limits of the low-alloy carbon steel in regions 1, 2, and 3 are 300, 280, and 250 Hv, respectively.

In recent years, low-alloy carbon steel has been used for line pipes in high-pressure H<sub>2</sub>S environments exceeding 1000 kPa (10 bar). However, it has become clear that SSC occurs in such harsh, sour environments.<sup>10-13)</sup> Furthermore, local hard zones (LHZs) (also called hard spots or hard layers) with a hardness of over 250 Hv were observed down to about 0.5 mm on the inner surface of SSC line pipes. Therefore, it is important to understand the SSC suscepti-

\* Ph.D, Senior Researcher, High Function Steel Research Dept., High Toughness Steel Research Lab., Steel Research Laboratories 20-1 Shintomi, Futttsu City, Chiba Pref. 293-8511

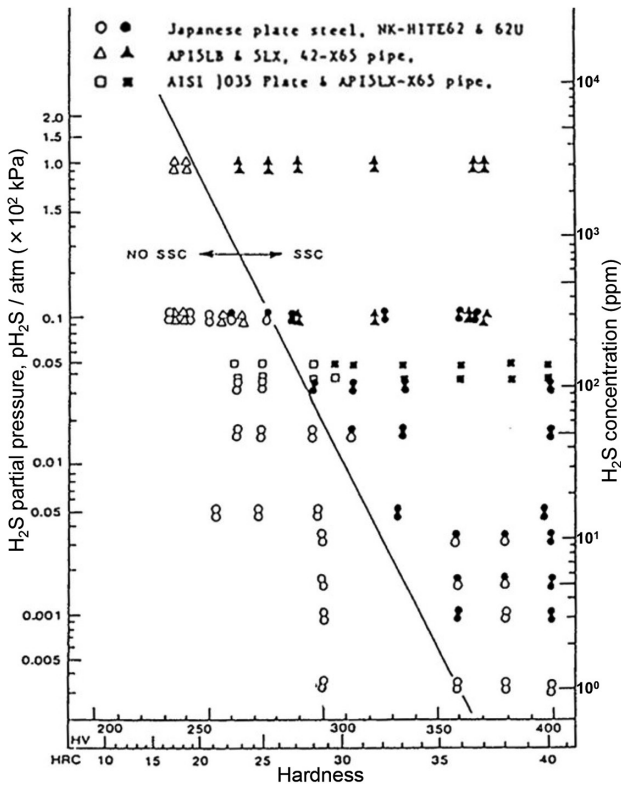


Fig. 1 Relations between hardness, H<sub>2</sub>S partial pressure, and SSC susceptibility<sup>7,8)</sup>

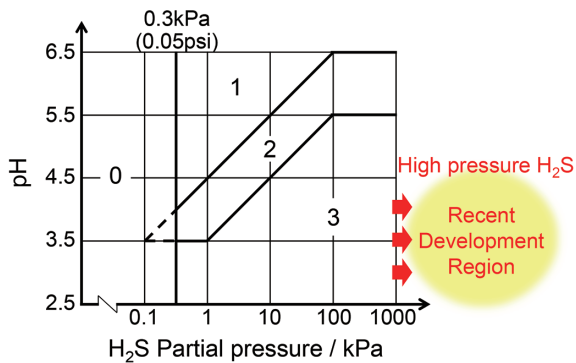


Fig. 2 Regions of environmental severity with respect to the SSC of carbon and low-alloy steels<sup>4)</sup>

bility and maximum acceptable hardness under high-pressure H<sub>2</sub>S environments, as well as the local microhardness and microstructure on the line pipe surface.

Low-alloy carbon steel has various microstructures, which are closely related to the hardness of the steel. **Table 1** shows schematic diagrams and names of the microstructures observed in low-alloy carbon steel used for line pipes. The name of the microstructure is defined based on the shape of ferrite and the precipitation form of cementite.<sup>14-16)</sup> The chemical composition of steel for line pipes is generally that of ultra-low carbon steel with a lower carbon concentration to bring out superior properties such as strength, toughness, and weldability. Therefore, lower bainite with plate-type bainitic ferrite and lenticular martensite observed in steels with relatively high carbon concentrations are not formed. Polygonal ferrite ( $\alpha_p$ ) is a mostly recrystallized ferrite with an equiaxed and polyhedral

Table 1 Schematic drawing of microstructures and nomenclatures<sup>14-17)</sup>

Schematics	Nomenclatures			This study
	Atlas for Bainitic Microstructures Vol.1	Ohmori et al.	BAINITE IN STEELS	
	$\alpha_p$ Polygonal Ferrite			$\alpha_p$ Polygonal Ferrite
	$\alpha_q$ Quasi-polygonal $\alpha$			$\alpha_q$ Quasi-polygonal $\alpha$
	$\alpha_w$ Widmanstätten $\alpha$ Acicular $\alpha$			$\alpha_w$ Widmanstätten $\alpha$ Acicular $\alpha$
	$\alpha_B$ Granular bainitic $\alpha$			$\alpha_B$ Granular bainite
	$\alpha_B^*$ Bainitic Ferrite	Upper bainite, BI	$\alpha_{ub}$ Upper bainite	$\alpha_{UB}(BI)$ Lath-type upper bainite (BI)
	$\alpha_B^*$ Lath-type BF	Upper bainite, BII		$\alpha_{UB}(BII)$ Lath-type upper bainite (BII)
	$\alpha_B^*$ Lath-type BF	Upper bainite, BIII		$\alpha_{LB}(BIII)$ Lath-type lower bainite (BIII)
	$\alpha_B^*$ Plate-type BF	Lower bainite	$\alpha_{lb}$ Lower bainite	$\alpha_{LB}$ Plate-type lower bainite
	$\alpha_{TM}$ Tempered Martensite			$\alpha_{TM}$ Tempered Martensite
	$\alpha^*$ Dislocated cubic Martensite			$\alpha^*$ Dislocated cubic Martensite

shape. Quasi-polygonal ferrite ( $\alpha_q$ ) is a ferrite with an irregular, variable shape that crosses over the  $\gamma$ -grain boundary. Widmanstätten/acycular ferrite ( $\alpha_w$ ) is a ferrite with characteristic lath/plate-like shape. Granular bainite ( $\alpha_B$ ) is a granular bainitic-ferritic structure with dislocated substructure but fairly recovered like “lath-less”. Bainite can be divided into four distinct types by the morphology of the bainitic ferrite ( $\alpha_B^*$ ), cementite ( $\theta$ ), and martensite-austenite constituent (MA). Lath-type upper bainite ( $\alpha_{UB}(BI)$ ) contains lath-type bainitic ferrite and retained austenite ( $\gamma_r$ )/MA formed within the lath (inter-lath). Lath-type upper bainite ( $\alpha_{UB}(BII)$ ) contains lath-type bainitic ferrite and cementite particles formed within the lath (inter-lath). If we focus on the shape of bainitic ferrite, it is upper bainite,<sup>15)</sup> but it is sometimes classified as lower bainite<sup>16)</sup> when attention is focused on the cementite precipitation position. In this report, to avoid confusion regarding terminology, this bainite is referred to as lath-type lower bainite ( $\alpha_{LB}(BIII)$ ).<sup>17)</sup> Dislocated cubic martensite is lath type martensite with a super saturated solid solution of carbon and high dislocation density.

In this paper, we present the results of our investigation into the hardness criterion and critical hydrogen content for SSC in high-pressure H<sub>2</sub>S environments in order to develop sour service line pipe steel that can be used in such conditions. We also identified the specific hardness of various microstructures obtained from low-alloy carbon steel for line pipes and compare it with the hardness criterion for SSC. Furthermore, we describe the manufacturing technology for sour-resistant line pipe steel preventing local hard zone for severe sour service using the thermo-mechanical control process (TMCP) including a controlled rolling and accelerated-cooling tech-

nology that achieves both excellent steel performance and production efficiency and ensures a microstructure that does not lead to SSC.

## 2. Investigation of Hardness Criterion for SSC in High-Pressure H<sub>2</sub>S Environment

To clarify the hardness criterion and critical hydrogen content for SSC, we prepared low-alloy carbon steels with various hardness values. Table 2 shows the chemical composition and carbon equivalent (Ceq) of the test steels.

### 2.1 Hardness criterion for SCC

To clarify the hardness criterion for SSC, we prepared tempered martensite steels with various hardness values. The 30-mm-thick steel ingots and with the chemical compositions shown in Table 2 were taken from cast slabs and subjected to the TMCP, and tempered in a laboratory, as shown in Fig. 3. First, the steel ingots were heated to 1250°C for austenite, controlled rolled to 8 mm steel plates, and acceleratedly cooled at a rate of 100°C/s or higher for transformation to martensite. Next, the controlled rolled and cooled steel plates were tempered at a temperature of 300 to 700°C and heat treated for 10 min to 4 h to produce tempered martensitic steels with various hardnesses, as shown in Fig. 4. The hardness of the

Table 2 Chemical compositions of plate materials used for laboratory evaluations

(mass%)					
Fe	C	Si	Mn	Others	Ceq
bal.	0.04   0.05	0.2   0.3	1.4   1.6	Ni, Cr, Mo, Nb, Ti	0.4

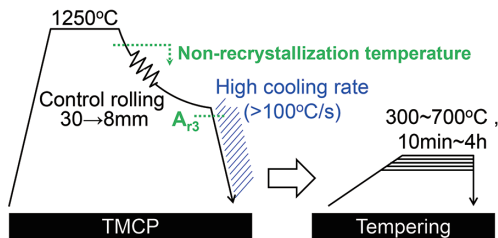


Fig. 3 Schematic drawing of TMCP and tempering conditions of the plate materials made in the laboratory<sup>17)</sup>

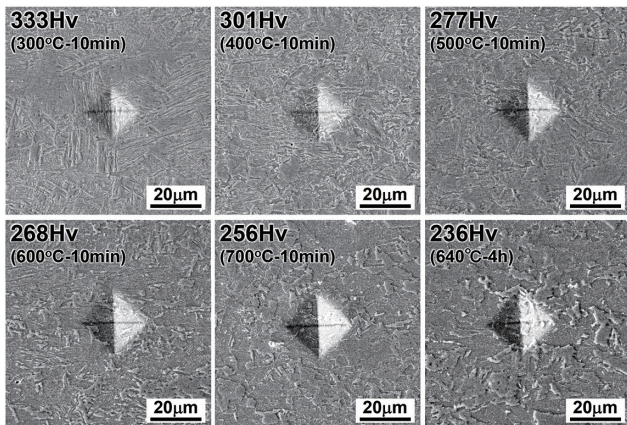


Fig. 4 Examples of SEM images and microhardness (0.1kg loads) of test materials<sup>17)</sup>

steel specimens decreases with the increase in the tempering temperature and tempering time. In this study, to evaluate the local maximum hardness of low-alloy carbon steel, the Vickers hardness test load was set at 0.1 kg, and the indent size measured during the test was reduced.

After the TMCP and tempering treatments, the specimens were tensile prestrained 2% to simulate the strain during cold forming of steel plates to pipes. For example, the 2% strain is equivalent to a pipe wall thickness/diameter (t/D) ratio of 0.02 during the forming of a steel pipe with an outside diameter (D) of 36 inches (914.4 mm) and a wall thickness (t) of 20 mm.

Figure 5 shows the results of the SSC test (four-point bend test in accordance with NACE TM0316). The applied stress in the four-point bend test in this study was 90% actual yield stress (AYS). In the figure, the red cross marks indicate the occurrence of SSC, and the blue circles indicate the results in which SSC did not occur. As shown in Fig. 5, SSC did not occur in the test materials that have a maximum microhardness less than 250 Hv (0.1 kg), regardless of H<sub>2</sub>S partial pressure. The results show that even if the H<sub>2</sub>S partial pressure increases from 1 bar to 16 bar (100 kPa to 1600 kPa), the upper hardness limit for SSC does not change. Similar results were reported by Shimamura et al.<sup>13)</sup> Figure 6 is obtained when the results of this study are combined with the effects of hardness and pH<sub>2</sub>S on SSC susceptibility reported by Taniyama et al.<sup>7)</sup> It was found that the hardness criterion for SSC in a sour environment decreases as the H<sub>2</sub>S partial pressure increases but remains constant at

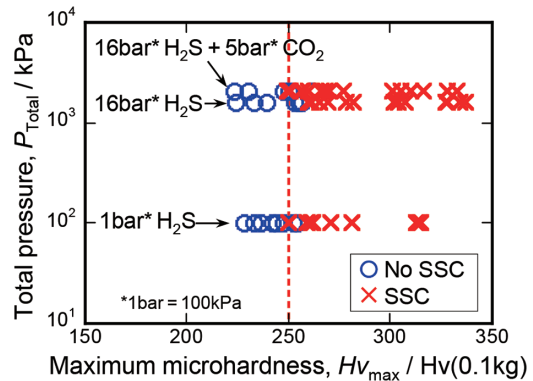


Fig. 5 Four-point bending test results regarding the relation between maximum microhardness (Hv<sub>max</sub>) and total pressure<sup>17)</sup>

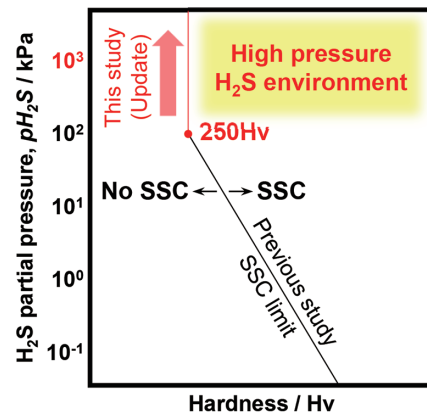


Fig. 6 Relations between hardness, H<sub>2</sub>S partial pressure up to 16 bar, and SSC susceptibility

250 Hv at or above 1 bar (100 kPa).<sup>17)</sup>

Here, we are faced with the industrial question of whether the value of hardness criterion for SSC remains unchanged even if the sour environment (hydrogen embrittlement environment) becomes even more severe and with the need for academic elucidation of the eigenvalue of 250 Hv and the SSC occurrence. For the former, this paper presents test results in a harsh environment where the critical hydrogen content was further increased. The latter elucidation of the mechanism involved is a topic for future research, but according to studies on the SSC occurrence mechanism by Asahi et al.,<sup>18)</sup> Yamane et al.,<sup>19)</sup> and Shimamura et al.,<sup>13)</sup> the occurrence of SSC is considered to be closely related to stress concentration due to corrosion (increase of the stress intensity factor (K value)) and to the fracture toughness of a material in the presence of H<sub>2</sub>S (i.e., under a severe hydrogen embrittlement environment) (fracture toughness value K<sub>ISSC</sub>, K<sub>IHP</sub> etc., of a hydrogen embrittled material).

### 2.2 Critical hydrogen content for SSC

Since SSC is a form of hydrogen embrittlement, the SSC susceptibility increases as the hydrogen content increases. Therefore, whether or not there is a critical hydrogen content to cause SSC in steels with a hardness criterion for SSC of 250 Hv or less is an extremely important issue from an industrial perspective. Here, we present the results of a laboratory investigation of SSC susceptibility when the hydrogen permeation content was increased as much as possible in a laboratory.

Kimura et al.<sup>20)</sup> measured the hydrogen content in a high-pressure H<sub>2</sub>S environment. The hydrogen permeation current measured by the electrochemical hydrogen permeation technique<sup>21,22)</sup> increases to about 40 μA/cm<sup>2</sup> as the H<sub>2</sub>S partial pressure or the CO<sub>2</sub> partial pressure increases. In the present study, to promote hydrogen absorption and to clarify the critical hydrogen content for SSC, we applied a potential of -1.2 V vs. silver-silver chloride electrode (saturated KCl) (hereafter referred to as Ag/AgCl) in an H<sub>2</sub>S environment where the hydrogen permeation was promoted, hydrogen was forcibly (cathodically) charged, and the hydrogen permeability was measured. **Figure 7** schematically illustrates the electrochemical hydrogen permeation method. The test solution used was the NACE solution A, which is the most severe test solution specified in the NACE TM0177 standard. The solution composition was 5.0wt%NaCl + 0.5wt%CH<sub>3</sub>COOH (initial pH 2.7), and the test gas was pure H<sub>2</sub>S gas at ambient pressure (1 bar H<sub>2</sub>S). The specimen area was 2 cm<sup>2</sup> and the specimen thickness was 1 mm. The surfaces of each specimen were mechanically polished and electrolytically polished. One side was electrolytically plated with nickel (Ni) in a Watt bath.<sup>22)</sup> Using a 0.1N NaOH aqueous solution as the solution on the hydrogen withdrawal side (anode side), the specimen was potentiostatically polarized at +0.148V vs. Ag/AgCl. After the passivation current density on the Ni plating reached 0.5 μA/cm<sup>2</sup> or less, the test solution was poured into the test cell on the hydrogen permeation side, and the hydrogen permeation test was started. The test temperature was 25±1°C, and the specific solution volume (ratio of the solution volume to the specimen surface area) was 100 ml/cm<sup>2</sup>. The hydrogen permeability (JL) (μA/cm)<sup>23,24)</sup> was calculated from the hydrogen permeation current density (J) and the specimen thickness (L), and the hydrogen permeability for non-charging and cathode charging were compared. The potential (corrosion potential) of non-charged specimen was about -0.6 V vs. Ag/AgCl.

**Figure 8** shows the change in the hydrogen permeability over time. The cathodic charge (hydrogen charge) at -1.2 V vs. Ag/AgCl

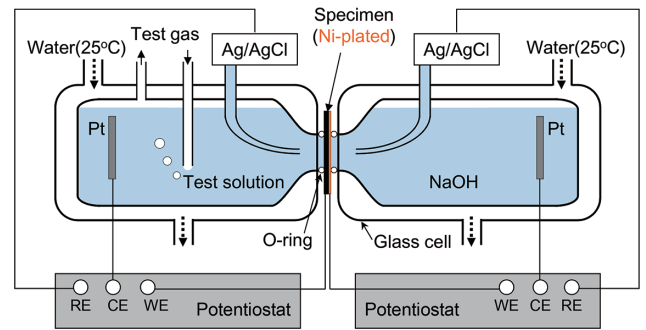


**Fig. 7** Schematic drawing of the test apparatus for hydrogen permeation<sup>17)</sup>

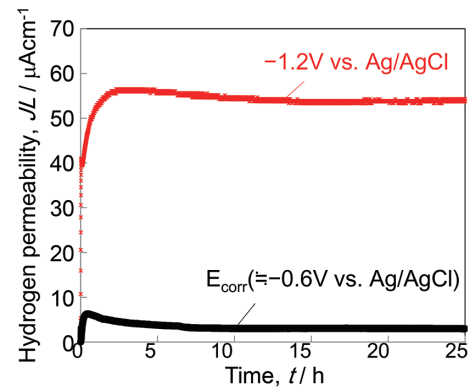


**Fig. 8** Time dependence of hydrogen permeability under NACE solution A ( $E_{corr}$ ) and NACE solution A with cathodic hydrogen charging (-1.2 V vs. Ag/AgCl)<sup>17)</sup>

increased the hydrogen permeability to over 50 μAcm<sup>-1</sup>. The hydrogen permeability under an H<sub>2</sub>S partial pressure of 15 bar (1 500 kPa) is reported to be about 20 μAcm<sup>-1</sup> (derived by multiplying the specimen thickness according to the results of Kimura et al.<sup>20)</sup>. Therefore, when the specimen is cathodically polarized at -1.2 V vs. Ag/AgCl in an H<sub>2</sub>S environment, the hydrogen permeability is much higher than the hydrogen permeability measured in a high-pressure H<sub>2</sub>S environment.

Next, to investigate the critical hydrogen content for SSC, steel specimens with various hardnesses were prepared in a laboratory and were four-point bend tested to evaluate their SSC susceptibility while being charged with hydrogen. The NACE solution A was used as the test solution. The applied stress was 90%AYS. In **Fig. 9**, the red cross marks indicate the occurrence of SSC, and the blue circles indicate the results in which SSC did not occur. The SSC test results under high pH<sub>2</sub>S (16 bar) were plotted around 20 μAcm<sup>-1</sup> according to a past report.<sup>20)</sup> As shown in Fig. 9, SSC did not occur in the specimens with 250 Hv (0.1 kg) or less, even when the hydrogen permeability was increased to 55 μAcm<sup>-1</sup>. The above results suggest that the critical hydrogen content is more than 55 μAcm<sup>-1</sup> for low-alloy carbon steels with 250 Hv (0.1 kg) or less or that SSC does not occur no matter how much the hydrogen content is increased (if the applied stress is 90%AYS as specified).

### 3. Specific Hardness and Hardness Criterion for SSC of Various Microstructures

To investigate the specific hardness of microstructures of low-alloy carbon steels for line pipes, we produced various microstructures in the laboratory and measured their hardness. Sheet-shaped

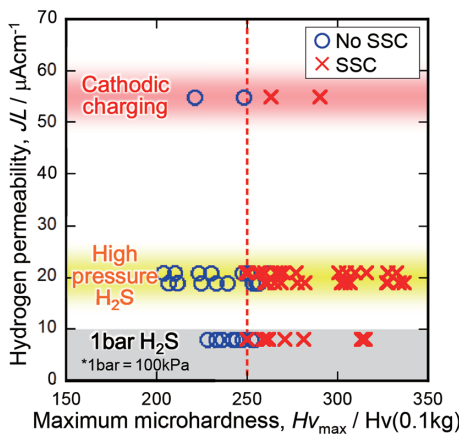


Fig. 9 4PB test results regarding the relation between maximum microhardness ( $Hv_{max}$ ) and hydrogen permeability<sup>17)</sup>

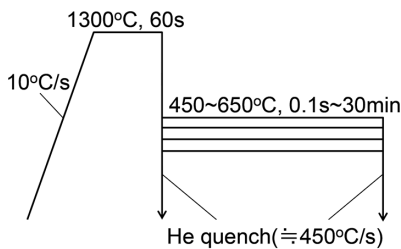


Fig. 10 Schematic drawing of the thermal cycle testing conditions used to measure the specific hardness of each microstructure<sup>17)</sup>

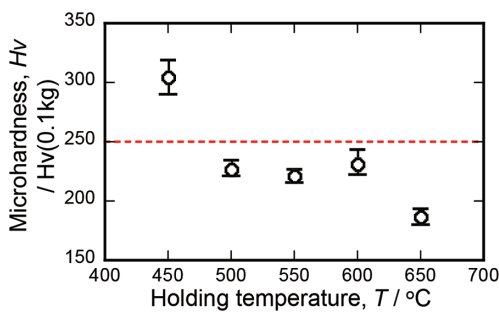


Fig. 11 Vickers hardness of the tested steels transformed at 450, 500, 550, 600, and 650°C<sup>17)</sup>

specimens with a thickness of 0.7 mm, a width of 10 mm, and a length of 80 mm were taken from low-alloy carbon steels with the chemical compositions shown in Table 2. The specimens were heat treated by a laboratory thermal cycle test, as shown in Fig. 10. The heat-treated specimens were measured for Vickers hardness and their microstructures were observed under an optical microscope and a scanning electron microscope (SEM).

Figure 11 shows the Vickers hardness of the specimens isothermally transformed at the respective temperatures. The hardness of the specimens transformed at 500°C or higher was less than 250 Hv (0.1 kg). Only the specimens transformed at 450°C exhibited a hardness of 250 Hv (0.1 kg) or higher.

Table 3 shows the schematics and nomenclatures of microstructures shown in Table 1, and the optical micrographs and SEM images of the test steels isothermally transformed at the respective temperatures. From the microstructures and substructures of the test steels, polygonal ferrite ( $\alpha_p$ ), quasi-polygonal ferrite ( $\alpha_q$ ), Widman-

stätten ferrite, or acicular ferrite ( $\alpha_w$ ) were observed in the test steels transformed at 650°C. Tempered martensite ( $\alpha_{TM}$ ) was observed in the test steel isothermally held at 650°C, but  $\alpha_{TM}$  was not transformed at 650°C but was transformed at a low temperature after it was isothermally held. Widmanstätten ferrite or acicular ferrite ( $\alpha_w$ ) and granular bainite ( $\alpha_B$ ) were observed in the test steel transformed at 600°C. Bainite or martensite was observed in the test steel that was transformed at temperatures below 550°C. When the microstructures were classified by the substructures observed in high-magnification SEM images, the bainite transformed at 550°C was classified into BI-type upper bainite ( $\alpha_{UB}(BI)$ ) with the retained austenite ( $\gamma_r$ ) or M-A formed inter-lath. The bainite transformed at 500°C was classified into BII-type upper bainite ( $\alpha_{UB}(BII)$ ) with cementite ( $\theta$ ) precipitated inter-lath. The microstructure transformed at 450°C was classified into lath-shaped lower bainite ( $\alpha_{LB}(BIII)$ ) or tempered martensite ( $\alpha_{TM}$ ) because cementite ( $\theta$ ) precipitation was observed intra-lath. The microstructure that exceeded 250 Hv (0.1 kg) was only that of the test steel transformed at 450°C, similar to the LHZ that was considered as the cause of SSC in the actual environment. Lath-shaped lower bainite ( $\alpha_{LB}(BIII)$ ) or tempered martensite ( $\alpha_{TM}$ ) should be avoided in SSC-resistant line pipe steels. Therefore, quasi-polygonal ferrite ( $\alpha_q$ ), Widmanstätten ferrite or acicular ferrite ( $\alpha_w$ ), granular bainite ( $\alpha_B$ ), or lath-shaped upper bainite (BI type or BII type) are preferred as the microstructures of low-alloy carbon steel for line pipes with excellent SSC resistance. Here, it should be noted that as the proportion of diffusion-transformed ferrite increases, carbon may be concentrated in untransformed austenite to form hard phases such as martensite or M-A.

#### 4. SSC Susceptibility of Commercial Line Pipes

To investigate the SSC susceptibility of commercial line pipes, we produced API grade X52, X60, and X65 low-alloy carbon steels for line pipes. We evaluated their SSC performance in a harsh, sour environment that simulates a high-pressure  $H_2S$  environment. Slabs with the chemical compositions shown in Table 4 were continuously cast at a steel mill and were controlled-rolled and accelerated-cooled using the TMCP at a plate mill. Figure 12 schematically illustrates the TMCP conditions. Based on the laboratory evaluation results, the microstructure was controlled by optimizing the reheating austenitization temperature, rough rolling conditions, controlled rolling conditions, and accelerated cooling conditions. In particular, a mild accelerated cooling (MAC) process was applied to avoid the formation of lath-shaped lower bainite ( $\alpha_{LB}(BIII)$ ) or (auto-)tempered martensite ( $\alpha_{TM}$ ) during accelerated cooling. After the TMCP, the line pipe steel plate was pressed into the U shape and then into the O shape. The formed steel pipe was expanded in the circumferential direction in the UOE process into a steel pipe with an outer diameter (D) of 36 inches (914.4 mm) and wall thickness (t) of 20 mm. Since the wall thickness to pipe diameter (t/D) ratio is about 0.02, the calculated average strain due to pipe forming is 2%, the same as the pre-strain applied in the laboratory.

Figure 13 shows an example of an optical micrograph taken at a position 0.5 mm beneath the inner surface of the manufactured X65 sour-resistant line pipe. Controlled by optimizing the TMCP conditions like the MAC process, the microstructure consists of quasi-polygonal ferrite ( $\alpha_q$ ), Widmanstätten/acicular ferrite ( $\alpha_w$ ), and granular bainite ( $\alpha_B$ ). It is a homogeneous fine-grained microstructure with a hardness of less than 250 Hv (0.1 kg). Figure 14 shows the SSC test (four-point bend test) results of the commercial line pipes (X52, X60, and X65). The specimens were taken with the inner surface

Table 3 Schematic drawing of microstructures, nomenclatures, optical micrographs, and SEM images of tested steel materials

Schematics	Nomenclatures	Microstructure	
	$\alpha_p$ Polygonal Ferrite		
	$\alpha_q$ Quasi-polygonal $\alpha$		
	$\alpha_w$ Widmanstätten $\alpha$ Acicular $\alpha$		
	$\alpha_B$ Granular bainite		
<hr/>			
	$\alpha_{UB}(BI)$ Lath-type upper bainite (BI)		
	$\alpha_{UB}(BII)$ Lath-type upper bainite (BII)		
	$\alpha_{LB}(BIII)$ Lath-type lower bainite (BIII)		
	$\alpha_{TM}$ Tempered Martensite		

Table 4 Chemical compositions of actual line pipe steel used for SSC susceptibility evaluations<sup>17)</sup>

Steel	Fe	C	Si	Mn	Others	Ceq
X52	bal.	0.05	0.3	1.3	Cr, Nb, Ti	0.30
X60	bal.	0.05	0.3	1.3	Cr, Mo, Nb,	0.35
X65					Ti	

layer of the commercial line pipe steel intact. The maximum microhardness ( $Hv_{max}$ ) is the maximum value obtained when microhardness was measured at five points from the inner surface layer to 0.1

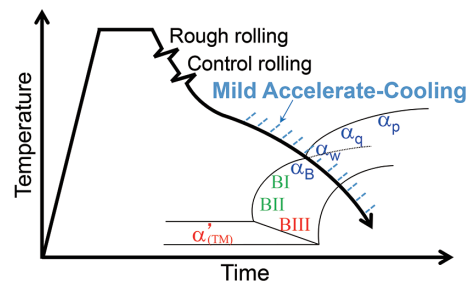


Fig. 12 Schematic drawing of optimized TMCP conditions of API grade X52, X60, and X65 line pipe steel manufactured in a mill

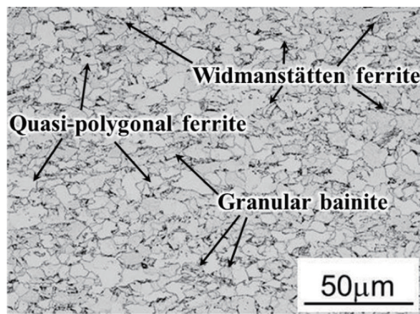


Fig. 13 Optical micrograph of the X65 sour-resistant line pipe (0.5 mm from inner surface)

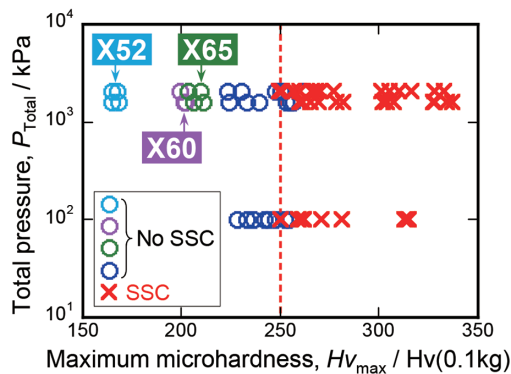


Fig. 14 4PB test results of X52, X60, and X65 line pipe steel regarding the relation between maximum microhardness ( $Hv_{max}$ )<sup>17)</sup> and total pressure

mm below. As shown in Fig. 14, SSC did not occur in the sour-resistant line pipe steel preventing local hard zone for severe sour service, even in a severely sour environment under high-pressure  $H_2S$ . The steels had the maximum microhardness controlled to less than 250 Hv (0.1 kg) and a properly controlled microstructure.

As described above, in this study, we investigated the optimal microstructure for sour-resistant line pipe steel preventing local hard zone that can be applied in a high-pressure  $H_2S$  environment from the viewpoint of SSC susceptibility and metallurgy. In other words, the hardness criterion for SSC is 250 Hv (0.1 kg) even in a high-pressure  $H_2S$  environment. The critical hydrogen content (hydrogen permeability) for SSC of low alloy carbon steel with a hardness of less than 250 Hv (0.1 kg) is more than  $55 \mu\text{Acm}^{-1}$  or is nonexistent (as far as the applied stress is 90%AYS). Furthermore, it was made clear that lath-shaped lower bainite ( $\alpha_{LB}$ (BIII)) or tempered martensite ( $\alpha_{TM}$ ) with a hardness exceeding 250 Hv (0.1 kg) should be avoided in low-alloy carbon steels for line pipes. It was also found that controlling the microstructure of SSC-resistant line pipe steels to quasi-polygonal ferrite ( $\alpha_q$ ), Widmanstätten/acicular ferrite ( $\alpha_w$ ), granular bainite ( $\alpha_B$ ), and upper bainite (BI or BII type) helps to keep the hardness below 250 Hv (0.1 kg) and ensure excellent SSC resistance.

## 5. Conclusions

In this paper, we investigated the hardness criterion and critical hydrogen content for SSC in a high-pressure  $H_2S$  environment, with the aim of developing line pipe steel that can be used in a high-pressure  $H_2S$  environment. In addition, we organized the specific hardness of various microstructures obtained in low-alloy carbon steels for line pipes, clarified the microstructures in which SSC does not

occur, and manufactured sour-resistant line pipe steel preventing local hard zone for severe sour service by TMCP controlled rolling and cooling. The main results are described below.

- (1) Hardness criterion for SSC: Under  $H_2S$  partial pressures of 1 bar and 16 bar (100 kPa and 1 600 kPa), SSC did not occur in low-alloy carbon steels with a maximum microhardness of less than 250 Hv (0.1 kg), regardless of the  $H_2S$  partial pressure. In other words, even when the  $H_2S$  partial pressure increased from 1 bar to 16 bar (100 kPa to 1 600 kPa), the hardness criterion for SSC was 250 Hv (0.1 kg).
- (2) Critical hydrogen content for SSC: SSC did not occur when the hydrogen permeability was increased to a hydrogen content ( $55 \mu\text{Acm}^{-1}$ ) higher than in a high-pressure  $H_2S$  environment by potentiostatic cathodic charging in an  $H_2S$  environment where hydrogen permeation was promoted. In other words, the critical hydrogen permeability of line pipe steel controlled to a hardness of less than 250 Hv (0.1 kg) was found to be over  $55 \mu\text{Acm}^{-1}$ .
- (3) Specific hardness and hardness criterion for SSC of microstructure: Assuming low-alloy carbon steel for line pipes, a microstructure exceeding 250 Hv (0.1 kg), like LHZ, consisted of lath-shaped lower bainite ( $\alpha_{LB}$ (BIII)) with cementite ( $\theta$ ) precipitated intra-lath or of tempered martensite ( $\alpha_{TM}$ ). For this reason, lath-shaped lower bainite ( $\alpha_{LB}$ (BIII)) or tempered martensite ( $\alpha_{TM}$ ) microstructure should be avoided in sour-resistant line pipe steel preventing local hard zone for severe sour service.
- (4) Actual production of sour-resistant line pipe steel preventing local hard zone for severe sour service: A homogeneous fine-grained microstructure consisting of quasi-polygonal ferrite ( $\alpha_q$ ), Widmanstätten/acicular ferrite ( $\alpha_w$ ), and granular bainite ( $\alpha_B$ ) with a hardness of less than 250 Hv (0.1 kg) was obtained by properly controlling TMCP conditions, such as applying the mild accelerate-cooling (MAC) process. The manufactured steels for sour-resistant line pipe steel preventing local hard zone exhibited excellent SSC resistance even under a severe high-pressure  $H_2S$  environment.

## References

- 1) Asahi, H.: Hydrogen Embrittlement of Oil Country Tubular Good and Line Pipe Steels. Zairyo-to-Kankyo. 49, 201 (2000)
- 2) Omura, T., Kobayashi, K.: Hydrogen Embrittlement of Oil Country Tubular Goods and Line Pipes. Zairyo-to-Kankyo. 60, 190 (2011)
- 3) Tuttle, T.N.: Materials Performance. 13, 42 (1974)
- 4) National Association of Corrosion Engineers (NACE): Petroleum and Natural Gas Industries—Materials for Use in  $H_2S$ -Containing environments in Oil and Gas Production, NACE Standard MR0175/ISO 15156-2, NACE, Houston, TX, (2015)
- 5) National Association of Corrosion Engineers (NACE): Laboratory Testing of Metals for Resistance to Sulfide Stress Cracking and Stress Corrosion Cracking in  $H_2S$  Environments, NACE Standard TM0177, NACE, Houston, TX, (2016)
- 6) National Association of Corrosion Engineers (NACE): Four-Point Bend Testing of Materials for Oil and Gas Applications, NACE Standard TM0316, NACE, Houston, TX, (2016)
- 7) Taniyama, M.: Stress Corrosion Cracking of Pressure Vessels and Their Piping. High Pressure Institute of Japan, 1979, 135p
- 8) Omar, A.A., Kane, R.D., Boyd, W.K.: Factors affecting the Sulfide Stress Cracking Resistance of Steel Weldments, CORROSION81, NACE, 186 (1981)
- 9) Kermani, B.M., Harrop, D., Truchon, R.L.M., Crolet, L.J.: Experimental limit of sour service for tubular steels, CORROSION91, NACE, 21 (1991)
- 10) Hara, T., Fujishiro, T., Shinohara, Y., Hamada, M.: Development of Sour Resistant Line pipes, 2nd Conference & Expo Genoa 2018, European event for the Corrosion Prevention, Milano, NACE international Euro-

## NIPPON STEEL TECHNICAL REPORT No. 132 FEBRUARY 2025

- pean Area, (2018)
- 11) Fairchild, P.D., Newbury, D.B., Anderson, D.T., Thirumalai, S.N.: Local Hard Zones in Sour Service Steels, Proceedings of the ASME 2019 38th International Conference on Ocean, Offshore and Arctic Engineering, Glasgow, OMAE, OMAE2019-96593, (2019)
  - 12) Newbury, D.B., Fairchild, P.D., Prescott, A.C., Anderson, D.T., Wasson, J.A.: Qualification of TMCP Pipe for Severe Sour Service: Mitigation of Local Hard Zones, Proceedings of the ASME 2019 38th International Conference on Ocean, Offshore and Arctic Engineering, Glasgow, OMAE, OMAE2019-96614, (2019)
  - 13) Shimamura, J., Izumi, D., Igi, S., Ishikawa, N., Ueoka, S., Ihara, K., Kondo, J.: Material Design for Grade X65 UOE Sour Linepipe Steels with SSC Resistant Property, Proc. 29th Int Offshore and Polar Eng Conf, Honolulu, ISOPE, 4209-4214 (2019)
  - 14) Bainite Research Subcommittee, Basic Research Group, ISIJ: Collection of Steel Bainite Micrographs-I. The Iron and Steel Institute of Japan, Tokyo, 1992
  - 15) Ohmori, Y., Ohtani, H., Kunitake, T.: The Bainite in Low Carbon Low Alloy High Strength Steels, Transactions of The Iron and Steel Institute of Japan. 11, 250-259 (1971)
  - 16) Bhadeshia, H.D.K.H.: Bainite in Steels—Second edition. IOM Communications Ltd., London, (2001)
  - 17) Fujishiro, T., Hara, T., Shinohara, Y., Hamada, M.: Sour-Resistant Line pipe for High-Pressure H<sub>2</sub>S Sour Service, Proc. of the 30th International Ocean and Polar Engineering Conference, Virtual, ISOPE, 2020-10, Paper No. ISOPE-I-20-4113
  - 18) Asahi, H., Ueno, M.: Evaluation of Cracking Susceptibility of Steels in Humid Hydrogen Sulfide Environment. Under Stress Corrosion Evaluation Subcommittee Symposium, The Iron and Steel Institute of Japan, 11-20 (1991)
  - 19) Yamane, Y., Motoda, K., Kurahashi, H., Nakai, Y.: Stress Corrosion Cracking Behavior of Low Alloy Steel in Sulfide Environment. Kawasaki Steel Technical Report. 17 (2), 178-184 (1985)
  - 20) Kimura, M., Totsuka, N., Kurisu, T., Hane, T., Nakai, Y.: Effect of Environmental Factors on Hydrogen Permeation in Linepipe Steel, CORROSION85, NACE, 237 (1985)
  - 21) Devanathan, M., Stachurski, Z.: The mechanism of Hydrogen Evaluation on Iron in Acid Solutions by Determination of Permeation Rates, Journal of Electrochemical Society. 111 (5), 619-623 (1964)
  - 22) Yoshizawa, S., Tsuruta, T., Yamakawa, K.: Development of Nickel Plating Method in Electrochemical Measurement of Hydrogen Content in Steel, Boushoku-Gijutsu. Japan Society of Corrosion Engineering. 24, 511 (1975)
  - 23) Kushida, T., Kudo, T.: Hydrogen Disbonding of Stainless Clad Steels by Cathodic Current, Tetsu-to-Hagané. The Iron and Steel Institute of Japan. 75, 1508 (1989)
  - 24) Kushida, T., Kudo, T.: Effect of Cr, Mo and Ni on Hydrogen Embrittlement of Martensitic Steels. Zairyo-to-Kankyo. Japan Society of Corrosion Engineering. 41, 677 (1992)



Taishi FUJISHIRO  
Ph.D, Senior Researcher  
High Function Steel Research Dept.  
High Toughness Steel Research Lab.  
Steel Research Laboratories  
20-1 Shintomi, Futtsu City, Chiba Pref. 293-8511



Nobuyuki YOSHIMURA  
Ph.D, Senior Researcher  
Steel Products Research Dept.  
East Nippon R & D Lab.



Masahiko HAMADA  
General Manager  
Tubular Products Technology Div.  
Pipe & Tube Unit



Taro MURAKI  
Chief Manager  
Plate Technical Service & Solution Dept.  
Plate Technology Div.  
Plate & Construction Products Unit



Takuya HARA  
Ph.D  
Former General Manager, Head of Lab., Pipe & Tube Research Lab., Steel Research Laboratories  
Currently Specially Appointed Professor (Research), Tohoku University